# ENRICHMENT OF IONS IN AEROSOLS OF SALT SOLUTIONS DUE TO BUBBLE BURSTING

A THESIS

Presented to

The Faculty of the Division of Graduate

Studies and Research

by

Sherman J. Glass, Jr.

In Partial Fulfillment

of the Requirements for the Degree

Master of Science in Chemical Engineering

Georgia Institute of Technology

August, 1972

In presenting the dissertation as a partial fulfillment of the requirements for an advanced degree from the Georgia Institute of Technology, I agree that the Library of the Institute shall make it available for inspection and circulation in accordance with its regulations governing materials of this type. I agree that permission to copy from, or to publish from, this dissertation may be granted by the professor under whose direction it was written, or, in his absence, by the Dean of the Graduate Division when such copying or publication is solely for scholarly purposes and does not involve potential financial gain. It is understood that any copying from, or publication of, this dissertation which involves potential financial gain will not be allowed without written permission.

7/25/68

# ENRICHMENT OF IONS IN AEROSOLS OF SALT SOLUTIONS DUE TO BUBBLE BURSTING

Approved:

Chairman: Michael J. Matteson

Clyde Orr, Jr.

R. A. Pierotti

Date approved by Chairman: 7/21/72

## ACKNOWLEDGMENTS

The author is very grateful to Dr. Michael J. Matteson whose guidance and advice contributed largely to the successful completion of this work. He is also grateful to Dr. Kevin Beck whose aid in the use of the atomic absorption spectrophotometer was invaluable. The author wishes to thank Dr. Clyde Orr, Jr. and Dr. Robert A. Pierotti for taking time to review this work.

A special thanks are extended to Mrs. Joyce Williams and Mrs. Marie Laboon for their assistance in typing.

The encouragement and understanding expressed by the author's wife, Alana Elizabeth Glass, are deeply appreciated.

The author would also like to thank the Department of Health, Education, and Welfare for financial support during this research.

TABLE OF CONTENTS

TABLE OF CONTENTS (Continued)

# LIST OF TABLES

# LIST OF FIGURES

# NOMENCLATURE

| | |
|---|---|
| a | Acceleration |
| B | Dummy constant |
| C | Dummy constant of integration |
| dt | Change in time |
| dv | Change in velocity |
| E | Enrichment |
| F | Total force |
| $\ell$ | Displacement from a streamline |
| $\mu$ | Viscosity |
| $\mu$m | Micrometer |
| m | Mass |
| r | Radius of a particle |
| R | Radius of a streamline |
| $\rho$ | Density |
| St | Stokes Number |
| t | Time |
| u | Velocity |
| $u_o$ | Initial velocity |

# SUMMARY

It is well known that a large part of the soluble salts found in soil, rivers, and lakes comes from rain water. These salts are believed to originate as ocean spray carried into the atmosphere from the surface of the seas. Here, tiny bubbles come to the surface and fracture, sending upward aerosols which contain these salts. Studies have shown that the ratio of the ions present within these aerosols are considerably different from those found in the oceans. The purpose of this investigation was to examine the bubble-bursting process in an effort to determine what is influencing the change in ion ratio. This was done by simulating the bubble-bursting mechanism in very simple salt solutions of concentrations similar to those found in the ocean. Variables examined were concentration, ion character, particle size, and pH.

It was found that definite trends in enrichments of one ion species with respect to another in the aerosol phase are related to the ratios of ions in the bulk solution. Also affecting enrichment is the pH of the bulk solution. Greatest enrichment was found in the smaller aerosol particles which suggests that the thin film formed before a bubble collapses is the place where the enrichment is occurring. The results further point to the fact that the ionic double layer is a major factor in the enrichment process in that it influences the ionic equilibria in the thin film of a bubble.

# CHAPTER I

## INTRODUCTION

It is uncommon for one to observe a large area of the ocean's surface engaged in a foaming or bubble-bursting process. However, three to four percent of the sea is continually engaged in this process. In this whitecap area, approximately one hundred thousand bubbles break in a square meter each second and send aerosol droplets upward (1). This bubble-bursting process is of great meterological importance for at this air-sea interface a unique exchange of matter and energy take place.

The first investigator to suggest the ocean as a source of particles for the atmosphere was Aitken (2) who in 1881 proposed that a significant number of air-borne particles might originate at the surface of the sea and also be the source of cloud formations. Following Aitken's theory, many investigators examined the oceans for such a process and Jacobs (3) in 1937 suggested the bubble-bursting mechanism as the source. However, not until 1948 and Woodkock's (4) experiences with a "red tide" off the coast of Florida did the bubble-bursting mechanism re-emerge as a prominent theory for the source of atmospheric nuclei. This theory was then confirmed by the work of Aliverti and Lovera (5), Boyce (6), and Facy (7).

After the bubble-bursting mechanism was fairly well accepted as responsible for the atmospheric nuclei, an enormous amount of work was initiated to determine exactly what the mechanism of the bubble-burst involved. Blanchard (8) and his associates utilized high speed

photographic equipment to arrive at the actual process as shown in Figure 1. They determined that a bubble rises to the surface forming a thin shell which quickly ruptures sending upward droplets of the micron size range. After the rupture, the shell collapses producing a jet of water which soon separates into a few droplets in the millimeter size range.

Continued studies by Blanchard (8) and his associates uncovered a phenomena of charge separation caused by the bubble-bursting process in which most of the particles released by the bubble-bursting mechanism carry a net positive charge. It is suspected that this phenomena is the source of a large fraction of the charged particles found in the atmosphere. Also these charged particles are believed to be one cause of thunderstorm activity common to cloud formations.

In addition to the charge separation aspect of the bubble-bursting mechanism, this phenomena is also considered the origin of large amounts of ions found in the atmosphere. An estimate of between two and ten billion tons of sea-salt per year is believed transferred from the ocean to the atmosphere by this process (9, 10). Recently, attention has been drawn to the various ionic species involved in this mass transfer. The major reason for this concern has grown out of studies showing that the ratios of the ions present in the atmosphere in the form of clouds and in rainwater are considerably different from the ratios of the same ions in seawater. Several investigators (11, 12, 13, 14) have shown that during the process by which aerosol droplets are injected into the atmosphere, an ion fractionation takes place such that certain ions are enriched relative to others while going from the bulk phase to the disperse phase.

MacIntyre (11) has observed that, in general, ions of higher ionic

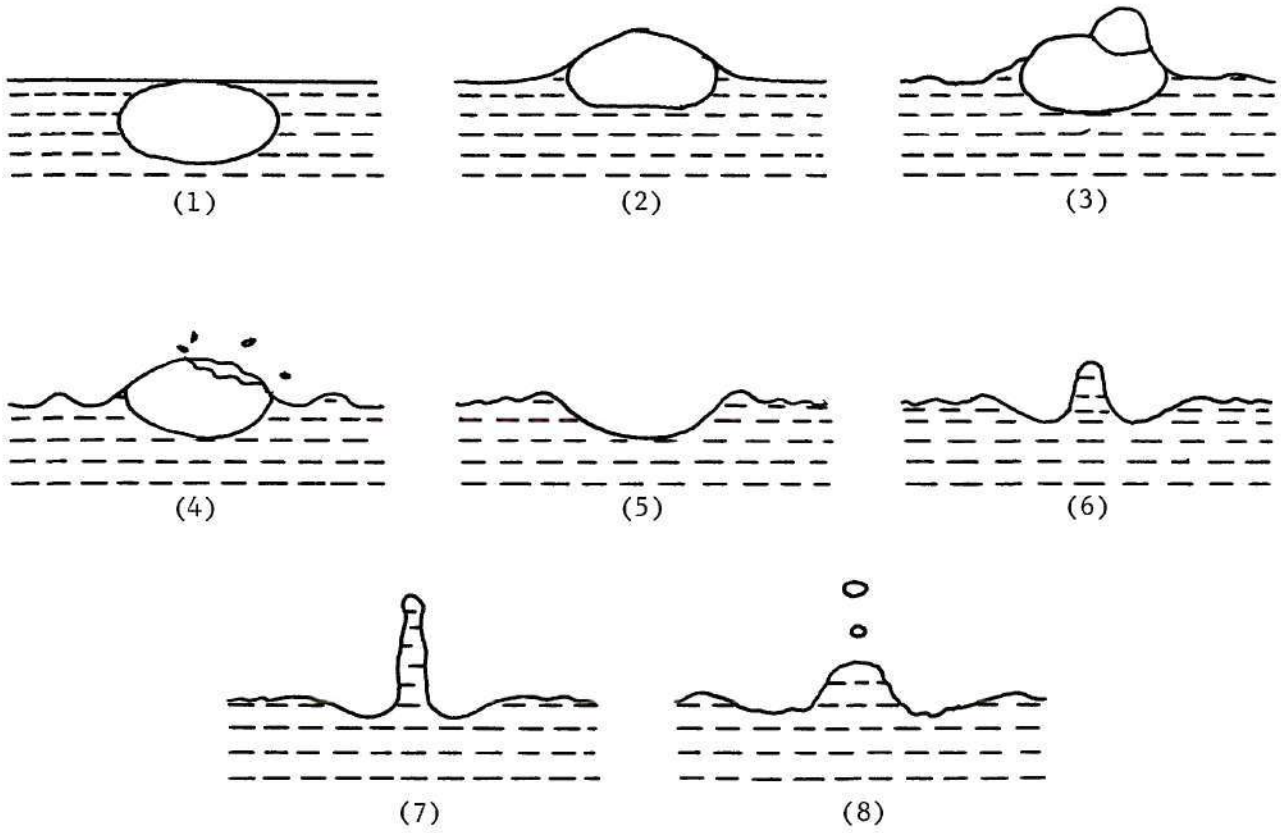


Figure 1. Mechanism of the Burst of an Air Bubble on the Surface of Water.

potential, or charge/mass ratio, are enriched relative to those of lower potential. For example, sulfate is enriched with respect to chloride and potassium with respect to sodium in going from the bulk to the disperse phase. Wilkness and Bressau (12) confirm MacIntyre's hypothesis by showing experimentally a decrease in $F^-/Cl^-$ in aerosols produced in the laboratory. Judson, et al., (13) show the same trend with $SO_4^=/Cl^-$ as do Bloch, et al., (14) with $K^+/Na^+$, $Br^-/Cl^-$, and $Ca^{++}/Na^+$. However, Kobajoski (15) and Sugawara (16) report $F^-/Cl^-$ ratios between ten and a thousand times higher in natural aerosols than those found in sea water. These findings suggest perhaps a more complex mechanism than that proposed by MacIntyre for ionic enrichment found in atmospheric aerosols.

The purpose of this investigation was to examine the bubble-bursting mechanism in an effort to determine what is influencing the change in ion ratio. This has been done by simulating the bubble-bursting process in very simple salt solutions. Aerosols produced by this process were collected by impaction and filtration devices. Analysis was made by conventional atomic absorption spectroscopy techniques. Ions studied are $Na^+$, $Mg^{++}$, $Li^+$, and $K^+$. Variables examined were concentration, ion character, particle size, and pH.

# CHAPTER II

## APPARATUS

A schematic representation of the experimental apparatus used for this research is presented in Figure 2. It consisted essentially of a boiling flask in series with a midget impinger and a filter holder and thus was quite simple in construction. The boiling flask was a standard 250 ml boiling flask, and was fitted with a cylindrical glass dispersion tube. This tube was 250 mm in length and 8 mm in diameter and was fitted with a gas sparger on one end.

Attached to the exit tube of the boiling flask was a midget impinger. This impinger consisted of a tube approximately 15 mm in diameter and 110 mm in length. Suspended within the tube was a probe to carry the gas flow from the boiling flask. Attached to the end of the probe was an orifice 1 mm in diameter. The probe and orifice were capable of being set at a variety of positions within the impinger tube.

Connected to the exit of the impinger tube was a Millipore filter holder which supports filters 47 mm in diameter. Filters used were Selas silver membrane filters of 0.22 μm pore size. This filter was chosen because of its uniformity in pore size and its high electrical conductivity. High electrical conductivity was important because the particles to be collected are most likely charged and a ground is required on the filter to prevent charge buildup which could hinder the collection process.

The air flow to the apparatus was regulated with a rotameter. This rotameter was calibrated against a wet-test meter as well as a

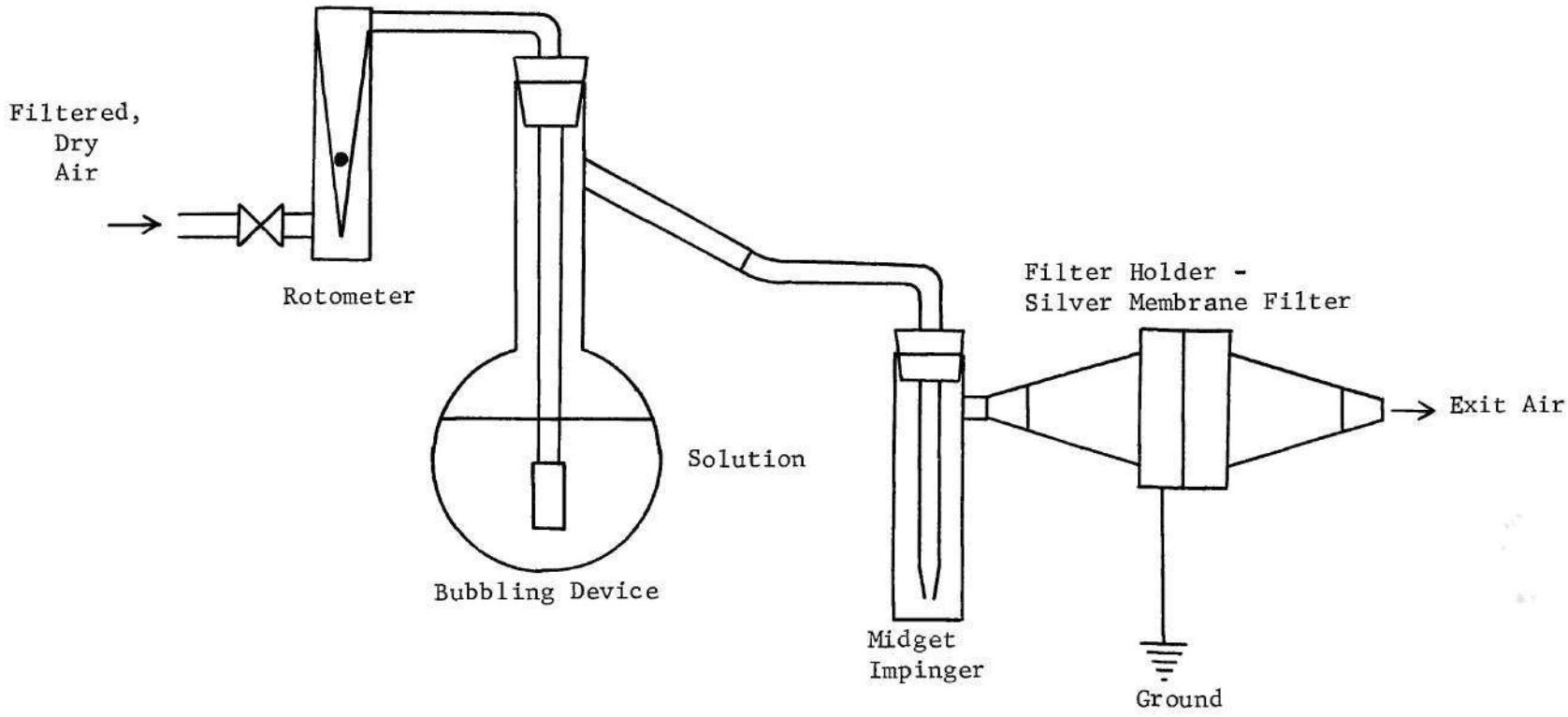


Figure 2. Appatarus.

standard rotameter. A calibration curve is presented in Appendix A.

All analyses were made using a Perkin-Elmer Atomic Absorption Spectrophotometer, Model 303. Attached to the flame absorption device was a concentration readout meter also manufactured by Perkin-Elmer. This meter is capable of giving direct readings of concentration when concentration is linear in relation to absorbance. For the ions examined, sodium, lithium, magnesium, and potassium, this relation was found to be true. Experimental graphs showing these linear relations are presented in Appendix B.

# CHAPTER III

# PROCEDURE

## Preparation of Bulk Solutions

All of the solutions used for analysis of the bubble-bursting mechanism were prepared using distilled, deionized water and reagent grade chemicals. In each case sodium chloride was three percent of the solution by weight. The other ion to be studied, magnesium, potassium, or lithium, was added in ratios as desired. The anion was usually in the chloride form although in one instance the sulfate was used. The ratios ranged from approximately 1/120 to 1/2 of ion studied to sodium ion. Standard procedures utilizing a Mettler balance and volumetric glassware were followed in preparing these solutions.

## Bubble-Bursting Simulation

Once a solution was prepared with the ratio of ions desired, it was placed in a 250 milliliter boiling flask. A gas dispersion tube was immersed into the flask. In an attempt to keep the bubble characteristics the same for all samples, the level of fluid within the boiling flask was kept constant as well as the depth of the gas dispersion tube. Also, the gas flow rate was held steady at 1.5 liters per minute for all runs. It was found that these conditions produced bubbles between 0.2 mm and 3.0 mm in diameter. A few bubbles larger than 3.0 mm were formed by attachment to the walls of the vessel. Although the actual distribution of bubble size was not found, it is believed that the bubble characteristics

were constant for each run due to the precautions previously discussed.

## Collection of Aerosols

In 1954, work by Newitt, et al., (17) showed that when a bubble bursts it produces aerosols that fall within two distinct size categories. One of these ranges is between a fraction of a micron and one hundred microns in diameter while the other is between 0.4 and 1.4 millimeters in diameter. As discussed in Chapter I, these size ranges are a by-product of the bubble bursting mechanism. The smaller range of aerosol sizes is formed when the bubble shell ruptures on the surface of the liquid. The larger range of aerosols comes from the spouting as the bubble collapses as shown in Figure 1.

Knowing that these aerosols are derived from two distinct and separate mechanisms which might have different fractionation processes, a collection arrangement was designed to collect each of these size ranges separately.

This was done by using an impaction device in series with a filter. Here, the entire flow of aerosol was sent through a tube fitted with a 1.0 mm orifice. At a specified distance from the orifice was a glass plate. For a constant rate of gas flow, aerosols of a specified diameter or greater have a momentum great enough to be thrown from the gas flow to the glass plate. Aerosols of a smaller mass stay in the gas flow and are carried on to a filter for collection. The impaction process is capable of discriminating between two distinct particle size ranges within certain limits. For each position of the orifice away from the retaining plate, there is a range of aerosols that are collected both in the

impinger as well as on the filter. Each time the orifice was positioned within the impaction tube, it was done with the aid of a five power optical microscope to enhance the accuracy of the placement. Table 1 gives size ranges collected *versus* impingement distances.

Table 1. Calculated Impingement Collection Ranges

| Impingement Distance, mm | Minimum Aerosol Diameter 100% Collected in Impinger, μm | Maximum Aerosol Diameter 100% Collected in Filter, μm |
|---|---|---|
| 1.0 | 3.6 | 1.3 |
| 2.5 | 5.6 | 2.1 |
| 5.0 | 8.0 | 3.0 |
| 7.5 | 9.8 | 3.9 |
| 10.0 | 11.2 | 4.2 |
| 15.0 | 13.9 | 5.2 |
| 20.0 | 16.0 | 6.0 |

Calculations used to develop Table 1 are presented in Appendix C. The calculations, however, are approximate since the tangential velocity of a particle and the medium are assumed to be the same as is the radius of curvature of the streamline with the impingement distance. These assumptions are reasonable at close impingement distances but become fairly crude for longer impingement distances. Although these calculations are somewhat inaccurate, the impingement process served very well the intention of separating the larger size aerosol fraction from the smaller aerosol fraction.

The aerosol passed by the impinger was collected on a silver membrane filter with pore sizes of 0.22 microns. This filter was grounded to prevent buildup of static charge which could possibly influence the collection process.

It was found that when bubbling dry air at 1.5 liters per minute, it took six to eight hours to build up enough aerosol deposit in the impinger and on the filter to allow for accurate analysis of the ion components.

## Methods of Analysis

At the end of each run, the silver membrane filter was removed from the filter holder and placed in 50 ml of distilled water to soak for twenty-four hours. The impinger tube and impinger probe were washed with distilled water and these washings were collected and diluted to 100 ml. The bulk solution was collected and diluted a thousand to one for analysis.

A Perkin-Elmer Atomic Absorption Spectrophotometer, Model 303, was used for analysis of the samples. Attached to the spectrophotometer was a digital concentration readout device also manufactured by Perkin-Elmer. This device is capable of giving direct readings of concentration when concentration is linear in relation to absorbance. For the ions examined, sodium, lithium, magnesium, and potassium, this relation was found to be true. Graphs of these relations as found experimentally are presented in Appendix B.

For each of the samples to be run, a set of standards of concentrations similar to those of the samples were made up and used to calibrate the concentration readout device. Once the spectrophotometer and concentration indicator were calibrated, it was a simple matter to determine the concentration of ions within each of the samples.

In each case, one ion was compared to sodium for change in ion concentration ratios. These data were reported for both the impinger and filter as percent sodium enrichment, E. Equation 1 shows the form of E

in comparison to potassium ion. The form for comparison to lithium ion or magnesium ion is identical.

$$E = \frac{\left(\frac{C_{Na^+}}{C_{K^+}}\right)_{Sample} - \left(\frac{C_{Na^+}}{C_{K^+}}\right)_{Bulk}}{\left(\frac{C_{Na^+}}{C_{K^+}}\right)_{Bulk}} \times 100\% \qquad (1)$$

Appendix D shows a sample calculation using Equation 1 as well as a relation of this E to the E of MacIntyre (11).

## Particle Size Analysis

In all runs except those explicitly designed to examine enrichment versus particle size, the impinger orifice was set 5 mm away from the glass impinger plate. At this setting all particles of eight microns in diameter or greater were caught in the impinger tube, while all particles of a three micron diameter or less were collected on the filter. The particles of a diameter between eight microns and three microns were gathered by both devices. This setting was thought to provide for an adequate split of the two ranges of aerosols produced by the bubble-bursting mechanism as previously discussed.

One study involved the examination of different size fractions of aerosols to determine if enrichment of ions were reflected in aerosol size. This was first examined by moving the orifice to different positions within the impinger tube, thus collecting different size fractions of the aerosols in the filter and midget impinger.

## pH Studies

In an attempt to determine if pH had an effect on the enrichment process due to the bubble bursting mechanism, a solution of magnesium chloride and sodium chloride was prepared with a mole ratio of magnesium ion to sodium ion of 0.074, the solution having a pH of 9.3. The solution was divided into four equal parts and the pH of each was adjusted using concentrated hydrochloric acid. The resulting pH valueswere 9.3, 6.1, 3.4, and 1.7. This procedure was used to ensure magnesium-to-sodium ratios that were equal in all solutions. Only the chloride concentration changed in this procedure and it was altered to an extent that was considered insignificant in the realm of this experiment.

Each of these solutions was bubbled using nitrogen rather than compressed air. The reason here being that when using dry air, carbon dioxide dissolves in solutions changing the pH to slightly acidic, and this phenomena could not be tolerated when examining the effect of pH.

Analytical procedures for the pH studies were identical to others using the atmoic absorption spectrophotometer.

# CHAPTER IV

## PRESENTATION OF RESULTS

### Enrichment Versus Concentration

Three different ions were examined as to their enrichment in comparison to the sodium ion. These were lithium, potassium, and magnesium. In each case a number of concentration ratios were examined. These ranged from as low as 0.01 to 0.5 in comparison to the sodium in the bulk. The sodium was held constant in all solutions at 3 percent sodium chloride by weight.

The results of these examinations are presented in Figures 3, 4, and 5. In each case except one the greater enrichment was found in the sample collected by the filter (Figure 3, $K^+/Na^+ = 0.18$). In that set of tests where the impinger shows more enrichment on the average than the filter, the results from the filter overlap those from the impinger, pointing to a possibility of greater enrichment.

In the set of samples where lithium is compared to sodium, a fifth set of samples was run with an ion ratio, $Li^+/Na^+$, of 0.01. However, in the impinger as well as the filter no lithium could be found. This pointed to a total enrichment of sodium at that concentration ratio.

Both $Mg^{++}$ and $K^+$ enriched compared to $Na^+$ at lower bulk ratios and this enrichment gradually decreased as the ratio of concentration in the bulk increased until the sodium became enriched as shown in Figures 3 and 4. Lithium, however, allowed great sodium enrichment at low concentration ratios which decreased as the concentration ratio of lithium to

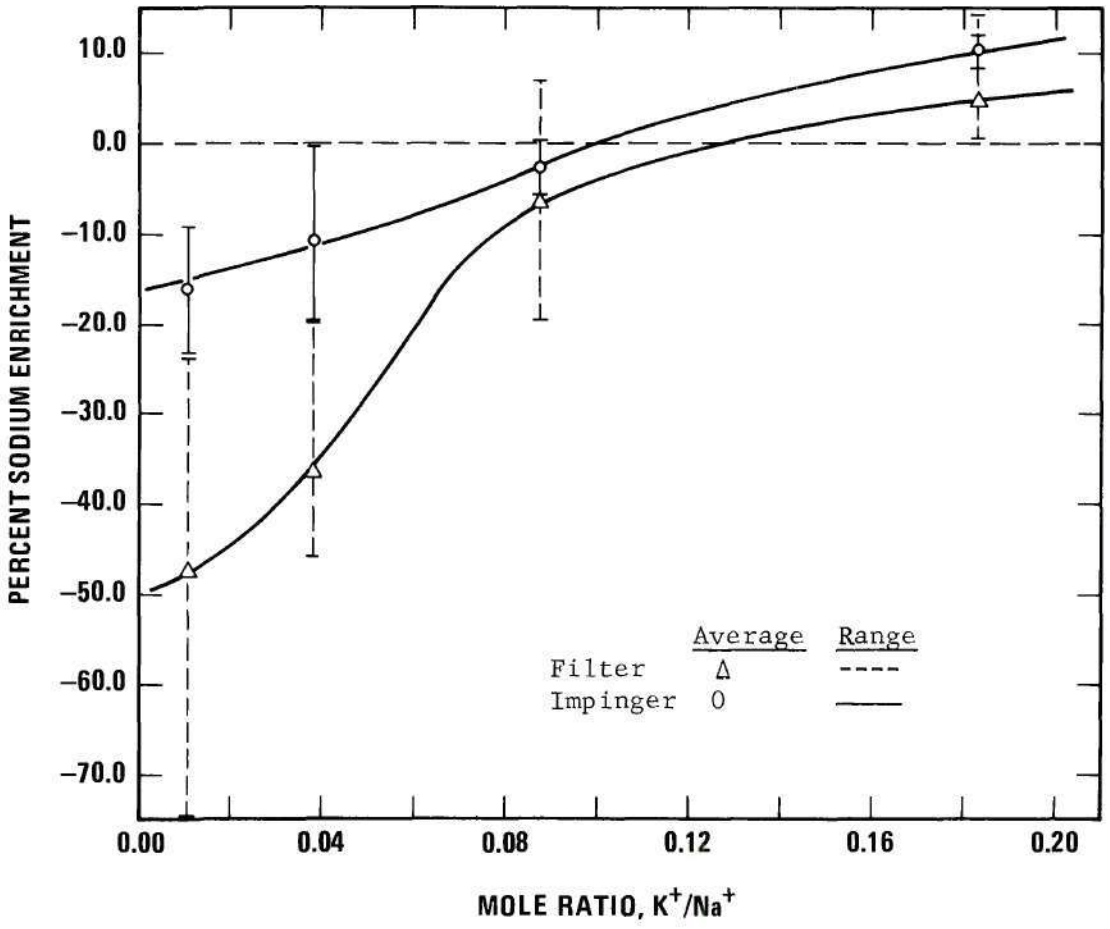


Figure 3. Enrichments in Potassium - Sodium Systems.

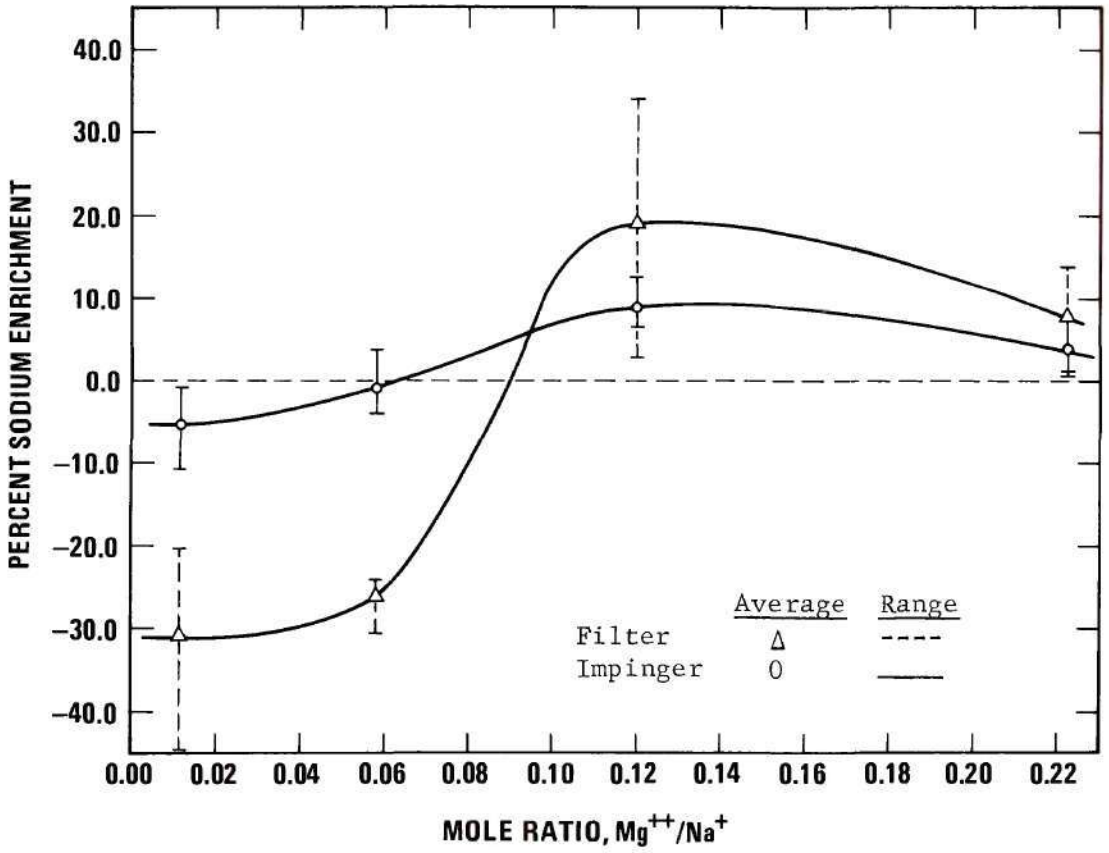


Figure 4. Enrichments in Magnesium - Sodium Systems.

sodium increased as shown in Figure 5.

The actual data points as calculated using Equation 1 are presented in Appendix E.

## Enrichment Versus pH

All aqueous solutions for bubble bursting examination were prepared with distilled, deionized water of a pH very close to 7.0. Since compressed, dry air was used for all runs except those specifically designed to study pH, the pH dropped slightly because of the carbon dioxide present. Here, carbon dioxide is dissolved in the bulk forming carbonic acid which gradually lowers the pH. Bulk solutions were found to have a pH as low as 6.4 after eight hours of run time which indicates only one hydrogen was dissociated from the carbonic acid molecule, thus leaving the bicarbonate ion in solution. It was felt since the biocarbonate ion has an ionic mobility so slow compared to the other negative ions studied, that it would rarely affect the enrichment process presumed to be taking place in the ionic double layer.

In testing the effect of pH, pure nitrogen was used in order to prevent pH changes due to the presence of carbon dioxide. It was found that an enrichment of sodium over magnesium increased as the pH changed from neutral in both directions as shown in Figure 6. The actual data points as calculated using Equation 1 are presented in Appendix E.

## Influence of Size Ranges on Enrichment

The influence of various particle size ranges on ion enrichment was tested by varying the depth of the impinger orifice within the impinger tube. This procedure allowed for collections of different size fractions

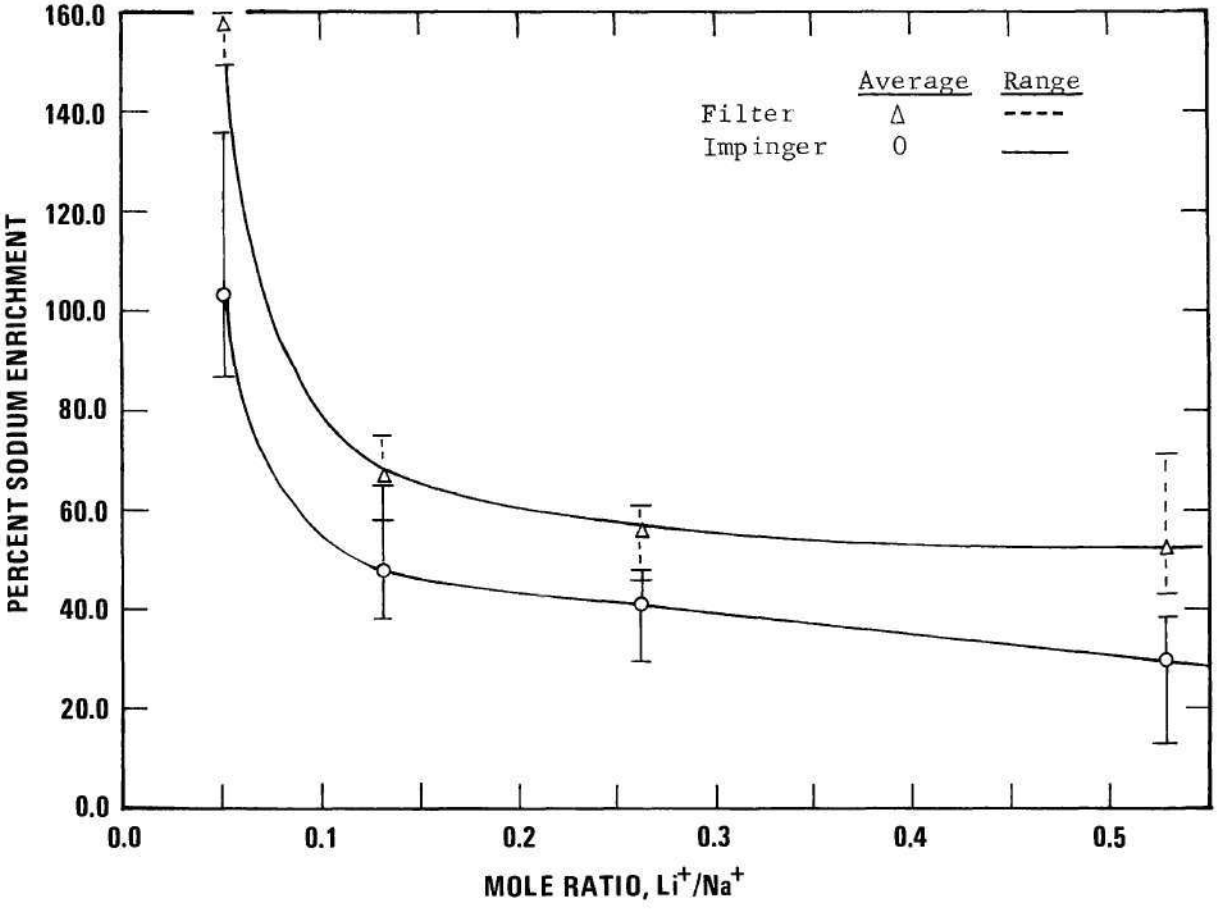


Figure 5. Enrichments in Lithium - Sodium Systems.

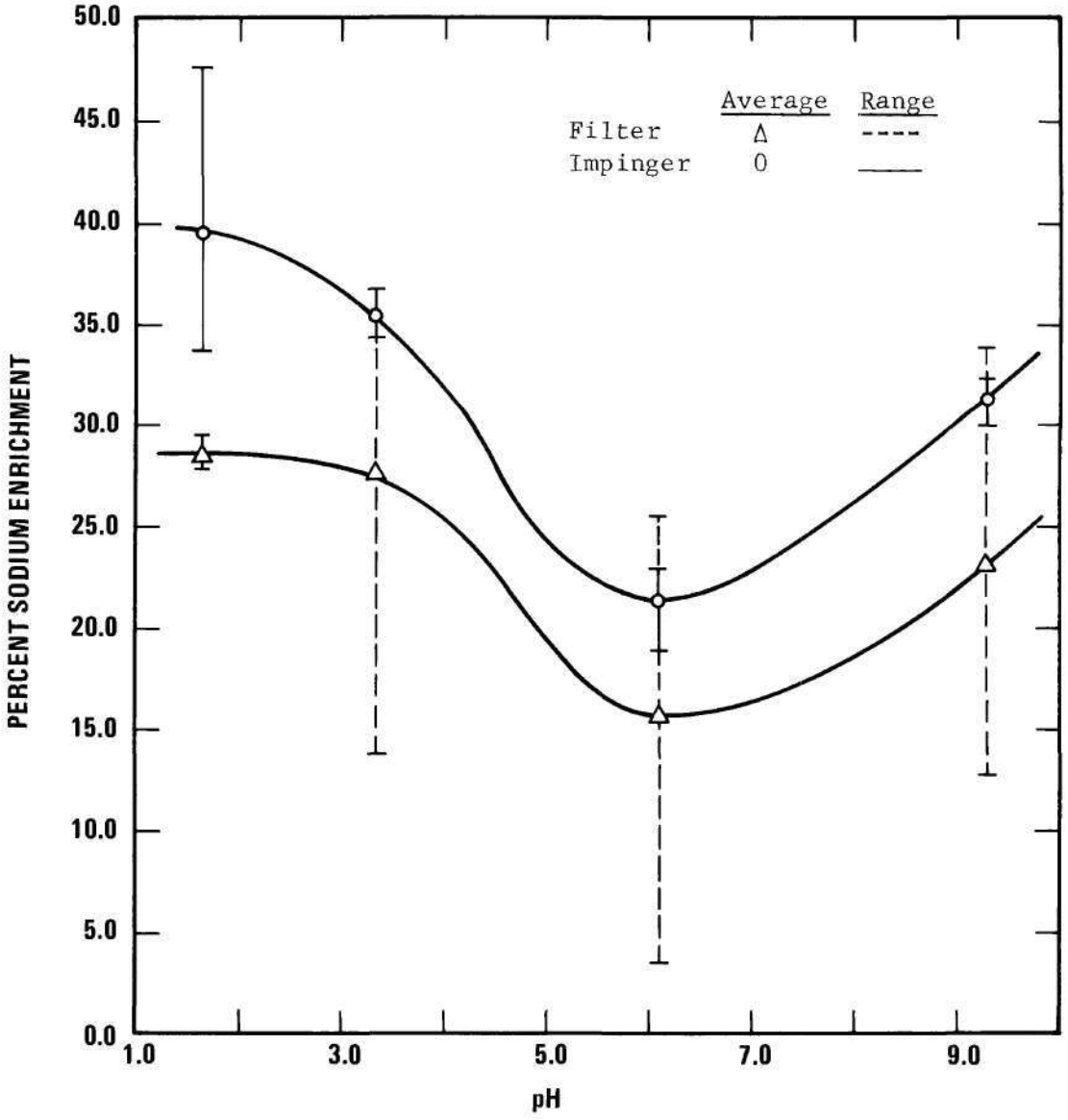


Figure 6. Effects of pH on a Magnesium - Sodium System.

of aerosols in the impinger and filter. These size fractions are presented in Table 1, and thus the enrichments are presented in Figure 7. These runs were made with a solution of magnesium chloride and sodium chloride. Here, the magnesium-to-sodium ion ratio in the bulk phase was 0.118. The data obtained from filter collections represent that particle size and smaller while the cutoff radii for the impinger collections represent that size and larger. Enrichment values from the lower sizes of particles collected by filtration appear to be greater than those from the larger particles collected by impingement. This is a result of the fact that the heavier, larger fraction contain those particles with almost no enrichment.

The actual enrichment for specific sizes alone would likely be much more exaggerated than the curves found experimentally for size range collections since the size range collections give integrated values. It does appear, however, that the smaller size ranges are the more enriched even though at very small sizes they seem to decrease.

The hump in the impinger collection data at around a radius of 5.6 microns is significant. Actual data points as calculated by Equation 1 are presented in Appendix G.

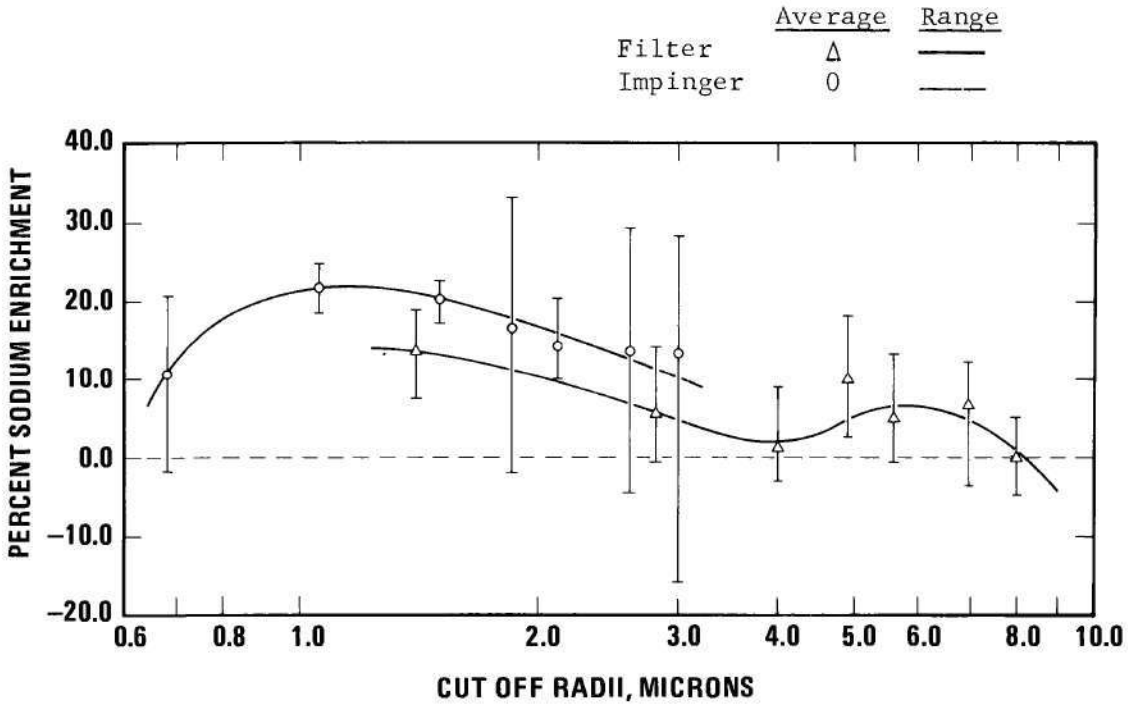


Figure 7. Enrichments Compared to Different Particle Size Fractions for a Magnesium - Sodium System.

# CHAPTER V

## DISCUSSION OF RESULTS

As previously discussed, MacIntyre (11), Wilkness and Bressau (12), and some other investigators report a trend of enrichment of salt in aerosols generated from the bursting of bubbles that follows an order of high ionic potential. For example, sulfate is enriched with respect to chloride as is potassium with respect to sodium in going from the bulk to the disperse phase. On the other hand, Kobajaski (15) and Sugawara (16) report opposite trends in natural aerosols for fluoride and chloride ions.

From the results presented in Chapter IV, it appears that this discrepancy can be explained. As is especially apparent with the studies conducted on magnesium and sodium and potassium and sodium systems, the degree of enrichment observed is highly dependent on ion ratios in the bulk phase. The lithium and sodium system also reflects this trend, however, it does not change enrichments from one ion to the other as do the other two systems.

It is gratifying to note that the enrichments found at concentration ratios close to sea water for the magnesium and potassium system are almost exactly the same as the maritime averages presented by Junge (18) for Western Europe. These are 36 percent potassium enrichment for a bulk mole ratio of 0.04 for $K^+/Na^+$ and 25 percent magnesium enrichment for a bulk mole ratio of 0.06 for $Mg^{++}/Na^+$.

Since the highest enrichment in almost every case was found in that aerosol fraction collected by the filter, it seems reasonable to

assume that the enriching process is occurring in the bubble bursting step where the smaller droplets are formed. This assumption is confirmed by the particle size study showing that the smaller particles are the more enriched, see Figure 7.

According to Newitt, et al., (17) as well as Blanchard (8), the small aerosols are formed in the bubble-bursting mechanism at the point where the thin film of a bubble on the liquid surface ruptures. This is shown in step 4 of Figure 1. At this point in the bubble-bursting mechanism, an extremely thin layer of solution is formed immediately before the bubble ruptures. It is in this thin liquid layer where the enrichment process appears to be occurring.

A well accepted theory of water molecule orientation is that of the electrical double layer set up at the gas-liquid interface of water. As presented by Loeb (19), at the surface of water a statistically significant number of the water molecules orient themselves with their oxygen atoms toward the surface and their hydrogen atoms down, or toward the solution. This formation sets up a net positive charge on the surface which then attracts negatively charged ions to satisfy it. These anions set up a negative shield over the positive field. This then attracts positive ions from the solution to satisfy this negative layer. These layers become more and more loosely held as the distance from the double layer increases. Also, the pH of the solution affects the orientation of the layers for the hydrogen ions and hydroxyl ions, if present, fill a portion of the positions as set up on the ionic double layer.

Now since these double layers are common on any liquid-air interface, it is highly likely that in the film formed in the bubble-bursting

mechanism there are two such layers. One facing the air above and one facing the gas of the bubble itself. Also, since this layer is extremely thin, it is likely that the ions in this region where the smaller aerosol droplets are formed are not characteristic of the bulk solution but, rather, are those ions held by the ionic double layer. Therefore, since those ions held in the double layer appear to be responsible for the ion enrichments found in aerosols, an examination of what selection process enables these ions to become attached to the double layer seems important.

Concentration, or availability of ions, appears as though it would play a major role in this selection process but, perhaps, equally important are ionic mobilities. Ionic mobility is the capability of an ion to travel in water as well as its ability to attach itself to water molecules. The ionic mobilities as reported by Davies (20) for the ions examined in this thesis are: sodium - 43.4 $cm^2$/volt·sec; magnesium - 45.5 $cm^2$/volt·sec; lithium - 33.3 $cm^2$/volt·sec; and potassium - 64.4 $cm^2$/volt·sec. These are for infinite dilutions at 18°C. Although these conditions are not exactly the same as those of the solution used in this experimentation, they do give the relative ease of movement through solutions for those ions as well as their ability to seek water molecules as riders.

It is the contention of this thesis that ionic mobility and ion capability for attachment to other molecules are the causes of the enrichments as previously found. It seems reasonable that an ion such as potassium with an extremely high ionic mobility might much more easily be drawn to an ionic double layer than a much slower ion such as sodium. It would then be this ability to "fit" in the ionic double layer that is responsible for enrichments seen at low concentration ratios of $K^+/Na^+$.

It appears that the ratio of $K^+$ to $Na^+$ in an ionic double layer might be relatively constant at around a $K^+/Na^+$ of 0.11 as seen in Figure 3, since at this ratio no enrichment appears to be found. Thus at high $K^+/Na^+$ ratios, $Na^+$ appears to be enriching but in actuality it is only the constant ratio of the ions in the double layer that is being reflected in the aerosols given off due to the bubble-bursting mechanism.

The same trend appears true of $Mg^{++}/Na^+$ although the ratio of enrichment appears equal at a $Mg^{++}/Na^+$ ratio of 0.08 as seen in Figure 4. As the mobilities become more nearly equal the enrichments do not seem so severe as is reflected in Figure 4 which shows $Mg^{++}$ and $Na^+$ not nearly so enriched as was the $K^+$ and $Na^+$ at low concentration ratios as shown in Figure 3.

Since lithium is very slow as compared to sodium, the opposite trend is expected and is found as shown in Figure 5. Here, it is felt that $Li^+$ is so slow as well as so highly hydrated that it has a difficult time getting into the ionic double layer and thus shows no enrichment. This trend could possibly change if $Li^+$ became the predominate ion as $Na^+$ was in all of the experiments carried out in the work. Here $Li^+$ would perhaps show up because it would be much more concentrated than $Na^+$.

If the ions present in the ionic double layer were always constant this ratio should be reflected in the aerosols given off from the double layer region. However, since these ratios varied, other factors must be affecting this double layer region. One of these is pH. Since a change in either the number of $OH^-$ ions or $H^+$ ions comes with a pH change, the occurrence of their presence in the double layer also changes thus changing the characteristic of the double layer. From Figure 6 it appears that

this change causes a shift in ion ratio present in the double layer which is reflected in the enrichments seen.

Although concentration has been somewhat neglected in this discussion it is thought that concentration is also a factor along with pH and ionic mobilities and it is the complex coupling of these three factors which account for the variety of enrichments as found by Junge (18) and others (15, 16). Though mobilities or the "fit" of an ion in a double layer are surely important in producing enrichments, it seems reasonable that major changes in concentration could cause these "fits" to be altered in character. This then might imply that there are more than one set of ion ratios comfortable in an ionic double layer and thus harmonic effects could occur with great changes in concentrations as well as bulk ion ratios. Similar effects were seen by Matteson (21) in measuring charge separation by atomization in bulk solutions similar to those studied here.

It is also interesting to note the oscillating trend of enrichments as a function of size range as shown in Figure 7. Similar effects were found by MacIntyre (11) for a phosphate and sodium system. These trends could possibly indicate that enrichments vary at different bubble film thicknesses. This could imply that at different double layer thicknesses configurations of ion "fits" change to give different enrichments of aerosols.

# CHAPTER VI

## CONCLUSIONS

The conclusions resulting from this work are summarized as follows:

1.) Enrichment between two ions going from the bulk phase to the dispersed phase by bubble bursting are highly dependent upon their ratio in the bulk phase.

2.) Enrichment between two ions going from the bulk phase to the dispersed phase are highly dependent on the pH of the bulk solution.

3.) Aerosols of salt solutions formed by the bubble-bursting mechanism are more highly enriched in the smaller size range. This indicates the enrichment process is taking place in the thin film formed before the bubble collapses as shown in step 4 of Figure 1.

4.) It appears that the ionic double layer as well as the mobilities of ions in solution are instrumental in the enrichment process.

# CHAPTER VII

## RECOMMENDATIONS

1. It is recommended that similar studies be performed on negatively charged ions such as fluoride and chloride to see if similar effects are found for negatively charged ions.

2. An extensive study of the effects of pH on enrichment might aid in a better explanation of the bubble bursting mechanism procedure of enrichment.

3. A study of enrichment changes as compared to different particle sizes rather than size fractions would be of great interest.

# APPENDICES

# APPENDIX A

## ROTAMETER CALIBRATION CURVE

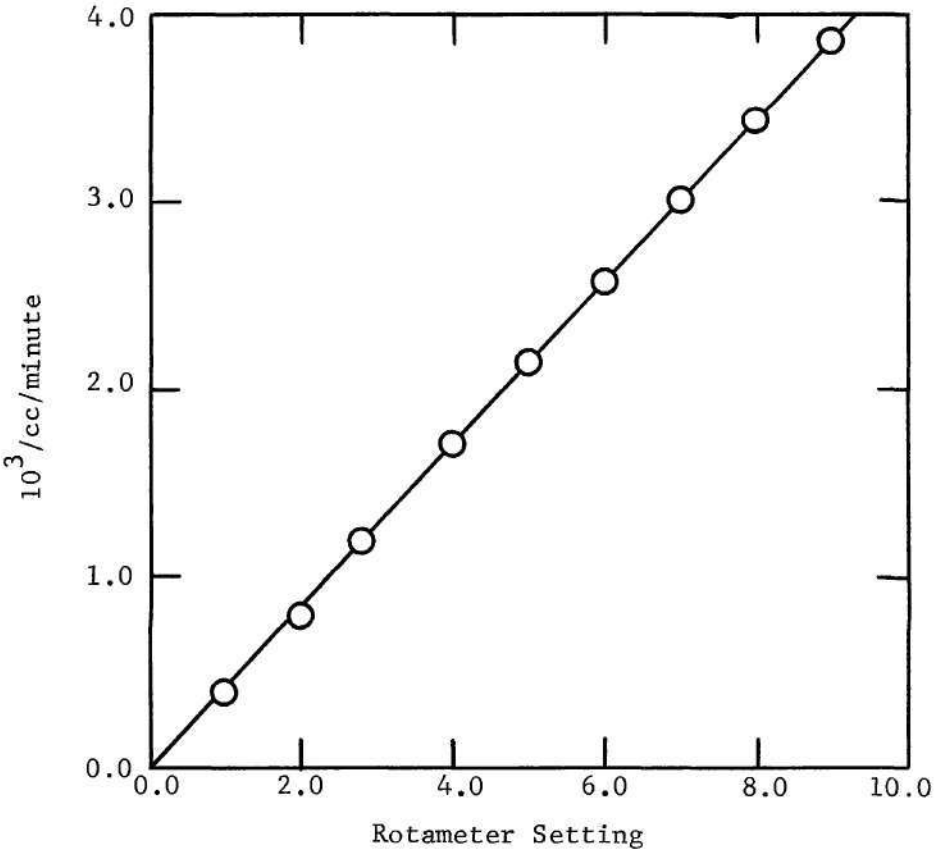


Figure 8. Filtered, Dry Air Rotameter Calibration Curve

# APPENDIX B

## CALIBRATION CURVES FOR ATOMIC ABSORPTION SPECTROPHOTOMETER

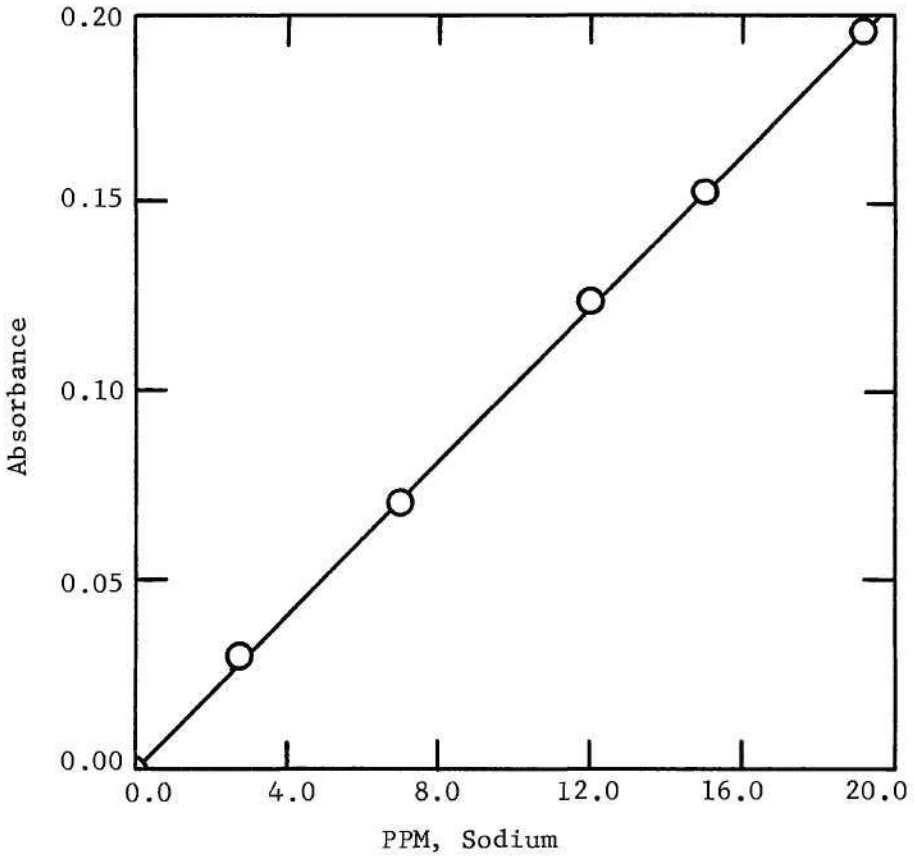


Figure 9. Absorption as Compared to Concentration for Sodium as Found Experimentally.

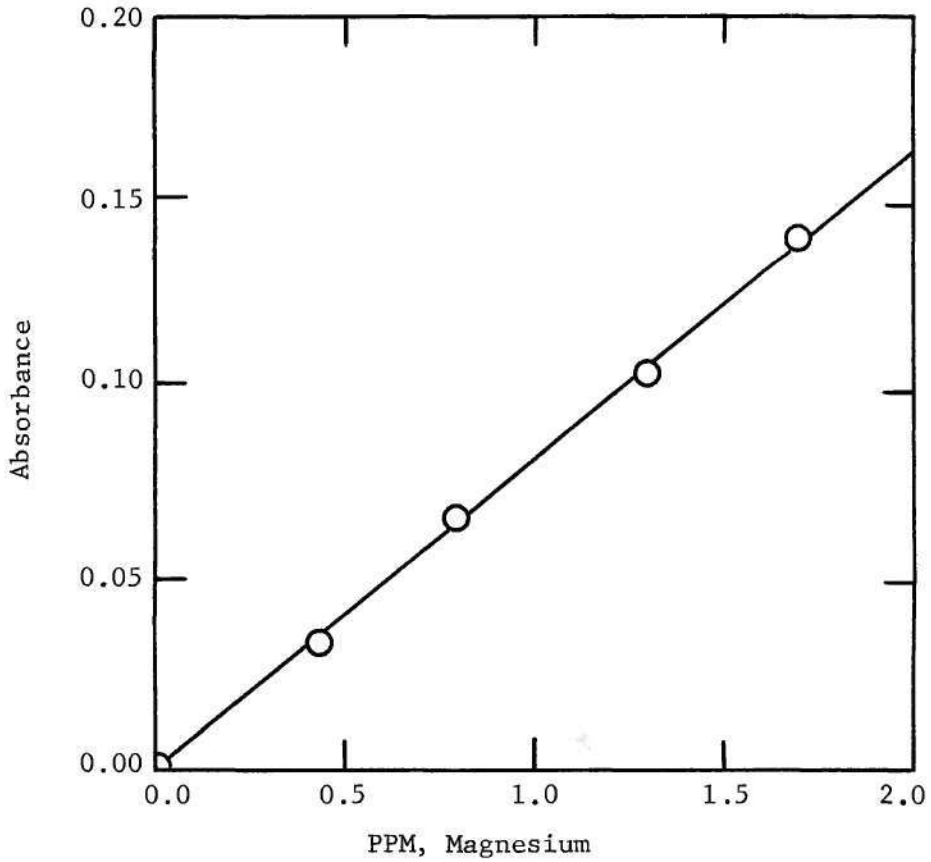


Figure 10. Absorption as Compared to Concentration for Magnesium as Found Experimentally.

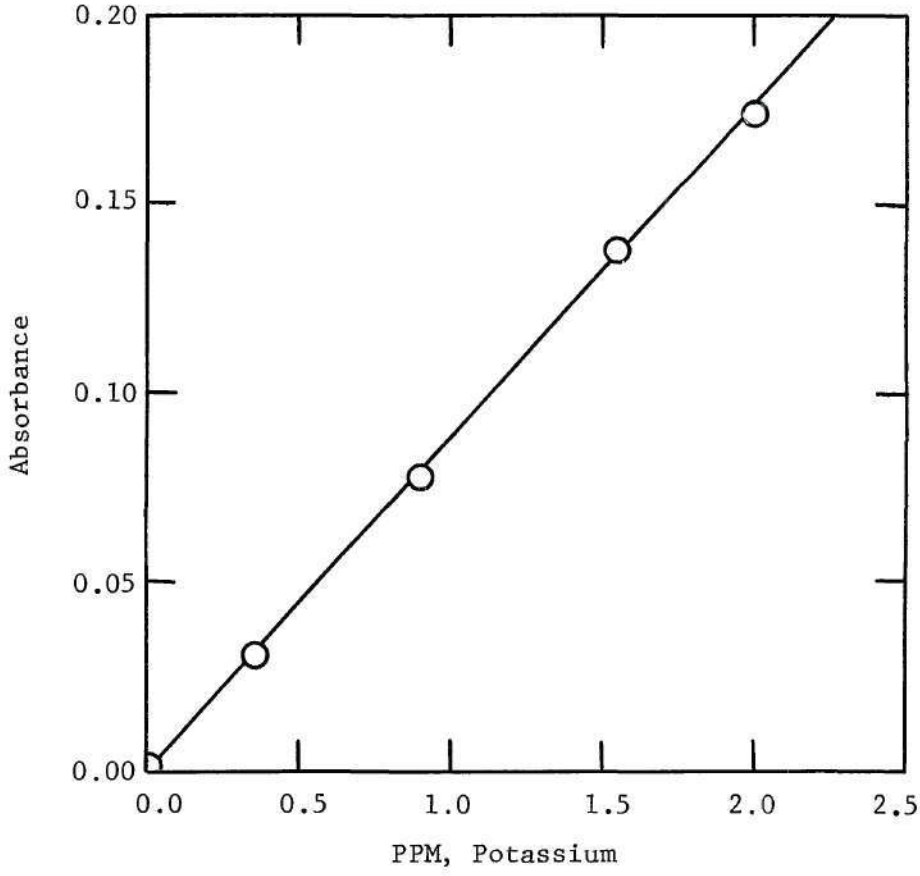


Figure 11. Absorbance as Compared to Concentration for Potassium as Found Experimentally.

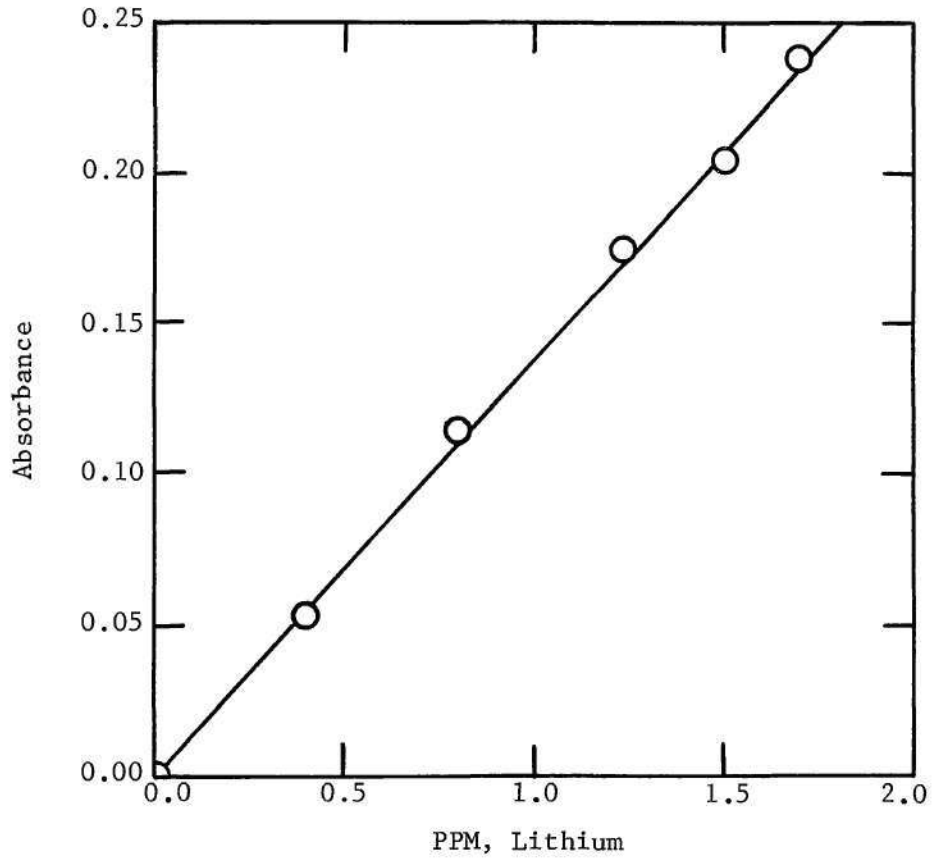


Figure 12. Absorbance as Compared to Concentration for Lithium as Found Experimentally.

# APPENDIX C

## IMPINGEMENT CALCULATIONS

In determing which particles in an air stream are collected by impingement, an equation summing the forces on the particle in the vertical direction is required. That is

$$F = ma - 6\pi\mu ur \tag{2}$$

These forces are the momentum due to gas flow and the stokes resistance opposing that momentum. For a particle to be removed from the air stream, the force of gravity must overcome the stokes drag or F, the total force on the particle in the downward direction must be zero or greater. In determining the smallest particle removed, F is set equal to zero and

$$ma = 6\pi\mu ur \tag{3}$$

or

$$\frac{a}{u} = \frac{B^{-1}}{m} \tag{4}$$

where

$$B = \frac{1}{6\pi\mu r} \tag{5}$$

Now since acceleration, a, is the change in velocity, du, with the change in time, dt, then

$$\frac{du}{udt} = \frac{B^{-1}}{m} \tag{6}$$

Rearrangement and integration yields

$$\ln u = \frac{-B^{-1}}{m} \cdot t + C \tag{7}$$

where C is a constant of integration. Since at time equal to zero, the initial velocity due to gravity is a constant, $u_o$, then

$$C = \ln u_o \tag{8}$$

and

$$u = u_o \, e^{\frac{-B^{-1}}{m} \cdot t} \tag{9}$$

The relaxation distance, $\ell$, or the distance a particle moves down and away from the streamline upon impingement is given by

$$\ell = \int_{t=o}^{t=\infty} u dt \tag{10}$$

as shown in Figure 13. This reduces to

$$\ell = Bmu_o \tag{11}$$

Dividing by the radius of curvature of the streamline, R, yields

$$\frac{\ell}{R} = St = \frac{Bmu_o}{R} \tag{12}$$

which is the stokes number.

Since $m = \frac{4}{3} \pi r^3 \rho$ and $B = \frac{1}{6\pi\mu r}$, then by substitution and rearrangement

$$St = \frac{2r^2 u_o \rho}{9\mu R} \tag{13}$$

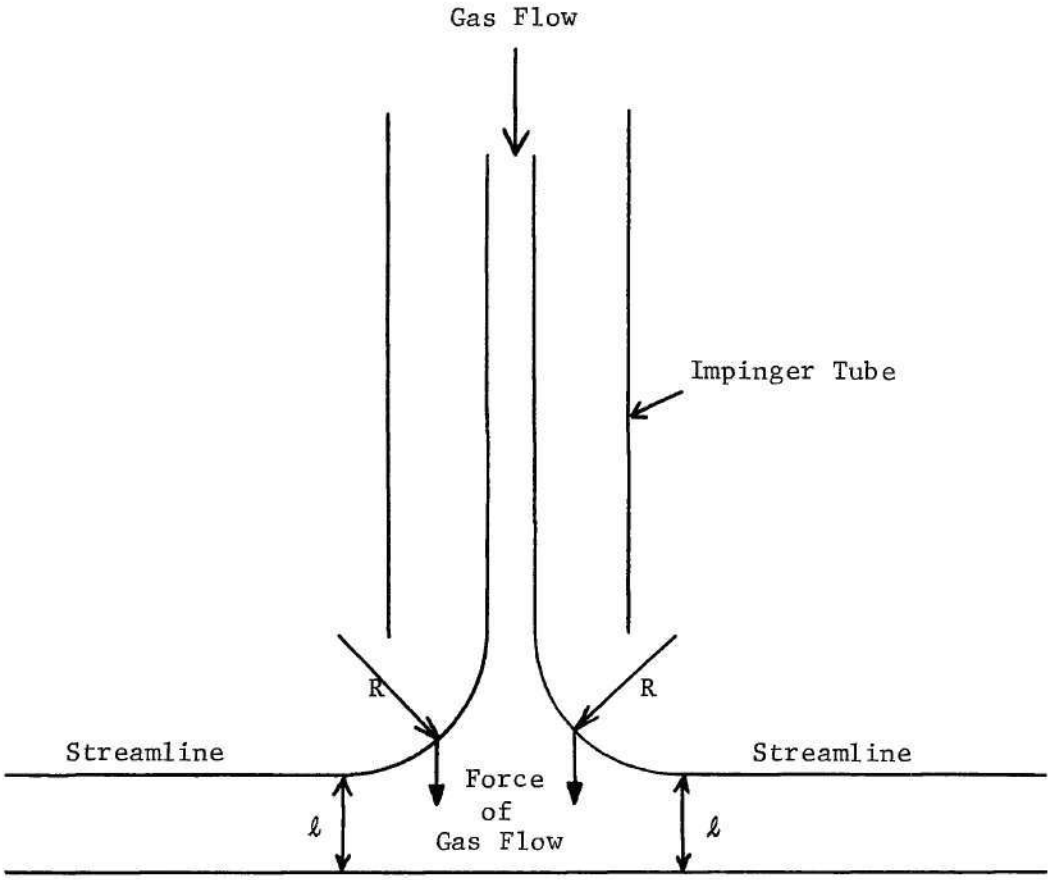


Figure 13. Flow Field in an Impingement Instrument

or

$$r^2 \rho \frac{u_o}{R} = St(\frac{9\mu}{2}) \tag{14}$$

Since the viscosity, $\mu$, of air at room temperature is $1.8 \times 10^{-4}$ poise and the density, $\rho$, of water is essentially one gram per cubic centimeter, then

$$r^2(\frac{u_o}{R}) = St\ (8.05 \times 10^{-4}) \tag{15}$$

The initial, vertical velocity, $u_o$, through the impinger due to gas flow is 31.8 meters per second and the radius of curvature of the air stream is assumed to be the impingement distance, 0.005 meters. Therefore,

$$\frac{u_o}{R} = 6.35 \times 10^3 \tag{16}$$

and

$$r^2 = St\ (1.27 \times 10^{-7}) \tag{17}$$

By rearrangement

$$r = 5.04 \sqrt{0.5 \cdot St} \tag{18}$$

Fuchs (22) presents data showing total impingement collection of particle at a $\sqrt{0.5St} = 0.8$ and total passage of particles at a $\sqrt{0.5St} = 0.3$. Therefore

$$r_{\text{Total Capture}} = 5.04(0.8) = 4.0\ \mu m \tag{19}$$

$$r_{\text{Total Passage}} = 5.04(0.3) = 1.5\ \mu m \tag{20}$$

Table 1 presents collection data for all impingement distances used in this work as calculated by the method presented here.

# APPENDIX D

## ENRICHMENT CALCULATIONS

### Sample Enrichment Calculation

To determine the enrichment of a sample where the $Na^{+}/Mg^{++}$ in the bulk is 3.87 and the $Na^{+}/Mg^{++}$ in the impinger is 4.27,

$$E = \frac{(Na^{+}/Mg^{++})_{Imp} - (Na^{+}/Mg^{++})_{Bulk}}{(Na^{+}/Mg^{++})_{Bulk}} \times 100\% \qquad (21)$$

is used. This is percent sodium enrichment for the sample. By substitution

$$E = \frac{4.27 - 3.87}{3.87} \times 100\% \qquad (22)$$

or

$$E = 10.4\% \qquad (23)$$

Thus, the sodium is enriched 10.4 percent in the impinger as compared to the bulk solution.

### MacIntyre's Enrichment*

MacIntyre (11) reports an enrichment, E, as $\frac{(P/Na)\ aerosol}{(P/Na)\ solution} - 1$ which is identical in form to Equations 1 and 21 except the 100 percent multiplier is not used. MacIntyre (11) also reports enrichments in terms of the ion other than sodium whereas this thesis standardized all

*Reference (11).

enrichment by reporting all in the form of sodium.

# APPENDIX E

## CALCULATED ENRICHMENTS FOR VARYING CONCENTRATION RATIOS OF $K^+/Na^+$, $Mg^{++}/Na^+$ and $Li^+/Na^+$

Table 2. Sodium Enrichments Found with Different Concentration Ratios of $K^+/Na^+$.

| Sample | Bulk Ratio ($K^+/Na^+$) | Impinger - % Sodium Enrichment | Filter - % Sodium Enrichment |
|---|---|---|---|
| 1 | 0.0107 | -9.2 | -25.3 |
| 2 | 0.0107 | -23.3 | -44.4 |
| 3 | 0.0107 | -16.1 | -75.9 |
| 4 | 0.0107 | - | -23.9 |
| 5 | 0.0375 | -7.9 | -19.5 |
| 6 | 0.0375 | -19.7 | -43.5 |
| 7 | 0.0375 | -15.5 | -36.4 |
| 8 | 0.0375 | 0.0 | -46.0 |
| 9 | 0.0875 | 0.1 | 6.9 |
| 10 | 0.0875 | -5.6 | -13.5 |
| 11 | 0.0875 | 0.0 | -19.3 |
| 12 | 0.0875 | - | 3.6 |
| 13 | 0.1830 | 3.1 | 9.9 |
| 14 | 0.1830 | 14.1 | 11.8 |
| 15 | 0.1830 | 0.6 | 11.2 |
| 16 | 0.1830 | 1.1 | 8.3 |

Table 3. Sodium Enrichments Found with Different Concentration Ratios of $Mg^{++}/Na^{+}$.

| Sample | Bulk Ratio ($Mg^{++}/Na^{+}$) | Impinger - % Sodium Enrichment | Filter - % Sodium Enrichment |
|---|---|---|---|
| 1 | 0.0113 | -0.8 | -46.7 |
| 2 | 0.0113 | -10.8 | -20.4 |
| 3 | 0.0113 | -4.6 | -25.0 |
| 4 | 0.0581 | -4.0 | -25.2 |
| 5 | 0.0581 | -2.9 | -24.1 |
| 6 | 0.0581 | 3.9 | -30.5 |
| 7 | 0.0581 | - | -24.2 |
| 8 | 0.1200 | 12.6 | 29.2 |
| 9 | 0.1200 | 6.5 | 34.0 |
| 10 | 0.1200 | 7.4 | 11.0 |
| 11 | 0.1200 | - | 2.9 |
| 12 | 0.2225 | 0.4 | 1.1 |
| 13 | 0.2225 | 7.4 | 8.5 |
| 14 | 0.2225 | 3.9 | 13.9 |

Table 4. Sodium Enrichments Found with Different Concentration Ratios of $Li^+/Na^+$.

| Sample | Bulk Ratio ($Li^+/Na^+$) | Impinger - % Sodium Enrichment | Filter - % Sodium Enrichment |
|---|---|---|---|
| 1 | 0.0083 | $Li^+$ Not Detectable | $Li^+$ Not Detectable |
| 2 | 0.0083 | $Li^+$ Not Detectable | $Li^+$ Not Detectable |
| 3 | 0.0083 | $Li^+$ Not Detectable | $Li^+$ Not Detectable |
| 4 | 0.0083 | $Li^+$ Not Detectable | $Li^+$ Not Detectable |
| 5 | 0.0513 | 135.4 | - |
| 6 | 0.0513 | - | 159.5 |
| 7 | 0.0513 | 94.5 | 159.5 |
| 8 | 0.0513 | 86.5 | 149.5 |
| 9 | 0.1310 | 46.1 | 71.5 |
| 10 | 0.1310 | 38.2 | 58.0 |
| 11 | 0.1310 | 65.2 | 75.0 |
| 12 | 0.1310 | 40.4 | 63.3 |
| 13 | 0.2620 | 48.6 | 60.3 |
| 14 | 0.2620 | - | 63.6 |
| 15 | 0.2620 | 42.3 | 53.2 |
| 16 | 0.2620 | 29.4 | 45.8 |
| 17 | 0.5290 | 12.8 | 71.0 |
| 18 | 0.5290 | 38.2 | 43.1 |
| 19 | 0.5290 | 31.8 | 46.9 |
| 20 | 0.5290 | 26.6 | 50.0 |

# APPENDIX F

## CALCULATED ENRICHMENTS OF SODIUM IN A SOLUTION OF $Mg^{++}$ AND $Na^{+}$ AT A MOLE RATIO OF .074 WITH VARYING pH.

Table 5. Sodium Enrichments Found with Different pH Values for a Solution of $Mg^{++}/Na^{+}$ Ratio of .074.

| Sample | pH | Impinger - % Sodium Enrichment | Filter - % Sodium Enrichment |
|---|---|---|---|
| 1 | 1.7 | 29.5 | 47.5 |
| 2 | 1.7 | - | 33.8 |
| 3 | 1.7 | 28.1 | 35.2 |
| 4 | 1.7 | 28.5 | 41.7 |
| 5 | 3.4 | 13.8 | 34.3 |
| 6 | 3.4 | 30.7 | 36.8 |
| 7 | 3.4 | 34.4 | 35.7 |
| 8 | 3.4 | 31.7 | - |
| 9 | 6.1 | 25.3 | - |
| 10 | 6.1 | 3.6 | 22.8 |
| 11 | 6.1 | 13.3 | 18.8 |
| 12 | 6.1 | 20.2 | 22.0 |
| 13 | 9.3 | 33.8 | 31.8 |
| 14 | 9.3 | 24.0 | 32.2 |
| 15 | 9.3 | 21.9 | 29.9 |
| 16 | 9.3 | 12.6 | - |

# APPENDIX G

## CALCULATED SODIUM ENRICHMENTS AT VARIOUS IMPINGER DISTANCES FOR A SOLUTION WITH AN ION RATIO OF $Mg^{++}/Na^{+} = 0.118$

Table 6. Calculated Sodium Enrichments at Various Impinger Distances.

| Sample | Impinger Distance (mm) | Impinger - % Sodium Enrichment | Filter - % Sodium Enrichment |
|---|---|---|---|
| 1 | 1.0 | 14.4 | 20.7 |
| 2 | 1.0 | 19.0 | -1.8 |
| 3 | 1.0 | 11.0 | - |
| 4 | 1.0 | 7.7 | 9.7 |
| 5 | 2.5 | 1.2 | 24.7 |
| 6 | 2.5 | 11.7 | 24.9 |
| 7 | 2.5 | 14.4 | 18.7 |
| 8 | 2.5 | -0.5 | 19.5 |
| 9 | 5.0 | -1.9 | 17.2 |
| 10 | 5.0 | 9.1 | 20.6 |
| 11 | 5.0 | -2.9 | 22.9 |
| 12 | 5.0 | 2.6 | 20.8 |
| 13 | 7.5 | 18.3 | -1.8 |
| 14 | 7.5 | 2.7 | 13.4 |
| 15 | 7.5 | 8.0 | 22.8 |
| 16 | 7.5 | 11.4 | 33.2 |
| 17 | 10.0 | 3.4 | 12.7 |
| 18 | 10.0 | 5.6 | 20.6 |
| 19 | 10.0 | -0.3 | 10.1 |
| 20 | 10.0 | 13.5 | 10.3 |
| 21 | 15.0 | 9.2 | 10.3 |
| 22 | 15.0 | -3.5 | 20.6 |
| 23 | 15.0 | 12.4 | 29.4 |
| 24 | 15.0 | 9.3 | -4.5 |
| 25 | 20.0 | - | 5.0 |
| 26 | 20.0 | 19.7 | - |
| 27 | 20.0 | 3.1 | 0.6 |
| 28 | 20.0 | -16.7 | -4.0 |

## REFERENCES


1. Blanchard, D. C., Saturday Review, 54 (1971), 60-63.

2. Aitken, J., Trans. Roy. Soc., Edinburgh, 30 (1881), 337-368.

3. Jacobs, W. C., Mon. Weather Rev., 65 (1937), 147-151.

4. Woodcock, A. H., J. Marine Res., 7 (1948), 56-62.

5. Aliventi, G. and Lovera, G., Pure and Applied Geophisics, 16 (1950), 133-135.

6. Boyce, S. G., Science, 113 (1951), 620-621.

7. Facy, L., J. Scientifique Meteorologie, 3 (1951), 62-68.

8. Blanchard, D. C., From Raindrops to Volcanoes, Garden City, N. Y., Doubleday & Company, Inc., 1966.

9. Blanchard, D. C., Progress in Oceanography (ed. M. Sears) 1, Chapter 2, 71-202, Pergamon Press, N. Y.

10. Eriksson, E., Part I, Tellus II. (1959), 375-403.

11. MacIntyre, F., Part IV, Tellus XXII. (1970), 451-461.

12. Wilkniss, P. E. and Bressan, D. J., J. Geophisical Res., 76 (1971), 736-741.

13. Judson, C. M., Lerew, A. A., Dixon, J. K. and Salley, D. J., J. Phys. Chem., 57 (1953), 916-923.

14. Bloch, M. R., Kaplan, D., Kertes, V. and Schnerb, J., Nature, 209 (1966), 396-397.

15. Kobajashi, S., "Geochemistry of Florine in Natural Waters," 68 pp., Suginyana Woman's College, Najoya, 1961.

16. Sugawara, K., Oceanogr. Mar. Biol. Ann. Rev., 3 (1965), 59.

17. Newitt, D. M. Dombrowski, N., and Knelasan, F. H., Trans. Instn. Chem. Engrs., 32 (1954), 244-261.

18. Junge, C. E., Air Chemistry and Radioactivity, New York, Academic Press, 1963.

19. Loeb, L. B., Static Electrification, Berlin, Springer - Verhag, 1958.

20. Davies, C. W., The Conductivity of Solutions, London, Chapman and Hall, LTD., 1930.

21. Matteson, M. J., J. Colloid Interface Sci., 37 (1971), 879-890.

22. Fuchs, N. A., The Mechanics of Aerosols, Oxford, Pergamon Press, 1964.